GLASS-FORMING REGION IN THE $GeSe_2$-In_2Te_3-GeTe SYSTEM AND SOME PHYSICOCHEMICAL PROPERTIES OF GLASSY ALLOYS

Lilia Aljihmani

University of Chemical Technology and Metallurgy
8 St. Kliment Ohridski Blvd., Sofia 1797
Bulgaria, l_aljihmani@uctm.edu (L.A.).

Received 20 June 2025
Accepted 18 September 2025 *DOI: 10.59957/jctm.v61.i3.2026.12*

ABSTRACT

For the first time, chalcogenide glasses from the $GeSe_2$-In_2Te_3-GeTe system are synthesized. Visual, X-ray diffraction, and electron microscopic investigations identify the glass-forming area, primarily located in the $GeSe_2$-rich region.

Differential thermal analysis determines the characteristic temperatures of phase transformations, including the glass transition temperature (T_g), crystallization temperature (T_{cr}), and melting temperature (T_m). Hruby's criterion is used to estimate the glass-forming ability (K_G). The chalcogenide glasses' density (d) and microhardness (HV) are measured. Compactness, elasticity modulus, and thermomechanical characteristics (micro-void volume (V_h) and formation energy (E_h)) are computed using the acquired properties. A thorough discussion and link between the glasses' properties and composition are established.

Keywords: glass-forming region, chalcogenide glasses, thermal properties, thermomechanical properties, physico-chemical properties.

INTRODUCTION

Chalcogenide glasses (ChG) have piqued researchers' interest due to their potential for use in various electronic fields. They combine some properties of crystalline semiconducting materials with the characteristic features of disordered systems [1, 2]. By altering the composition, adding a third element to binary chalcogenide glasses improves the likelihood of a wide range of features.

It has recently been shown that adding selenium enhances the corrosion stability of a tellurium layer [3]. Tellurium and selenium-based layers, therefore, represent attractive materials for devices utilizing amorphous to crystalline phase change. A great deal of scientific research is conducted on the potential for information recording in chalcogenide amorphous semiconductors and the convertible electrical switching over that is observed in certain of them [4 - 8].

The amorphous-crystalline phase transition is linked to photo structural alterations that have affected the optical characteristics of the chalcogenide layers (reflection, transmission, and absorption coefficients). The chalcogenide layer's information is recorded and removed using these procedures. In the field of micro- and optoelectronics, optical systems based on laser-induced phase changes between amorphous and crystalline states are promising.

In the near, mid, and far-infrared regions of the spectrum, chalcogenide glasses are among the most promising materials for fiber and thin-film waveguides [9 - 13]. Because chalcogenide glasses have good transmission in this wavelength range and provide an appropriate environment for the high-power emission of CO_2 lasers, researchers have concentrated their efforts primarily on reducing the transmission losses in this spectrum region [14]. For glasses based on Ge-chalcogenides (Ge-Sb-Se), the absorption coefficient is 0.029 cm^{-1} at 10.16 μm [15]. When Sb is replaced with

As, the absorption coefficient for the As-chalcogenide glass Ge-As-Se is 0.0143 cm^{-1} at 1.55 μm [16].

Other authors claim that the addition of Te up to 50 at. % to the chalcogenide glasses on a selenium basis can reduce optical losses in the 8 - 12 μm range [1, 17]. A study presents a germanium-rich selenium chalcogenide fiber with optical loss below 3 dB/m between 5.1-7.9 μm, minimizing at 6.61 μm. Its dispersion is ideal for mid-infrared supercontinuum generation [18].

Chalcogenide glasses are widely used in infrared optics because of their high refractive index and minimal optical losses, which enable efficient transmission and manipulation of mid-infrared light [17].

The current effort aims to outline the glass-formation region within the $GeSe_2$-In_2Te_3-GeTe system and explore the key properties of the newly generated ChG.

EXPERIMENTAL

The glass-forming region within the $GeSe_2$-In_2Te_3-GeTe system is outlined by the help of 27 samples with joint composition $(GeSe_2)_x(In_2Te_3)_y(GeTe)_z$, where x + y + z = 100 (Table 1).

The precursor compounds $GeSe_2$, In_2Te_3, and GeTe and glasses (4 g) from the $GeSe_2$-In_2Te_3-GeTe system are produced by direct monotemperature synthesis in vacuum-sealed quartz ampoules with a residual pressure of 1.10^{-3} Pa. Ge, Se, and Te with a purity of 5N (Fluka),

Table 1. Compounds used for outlining the glass formation region within the $GeSe_2$-In_2Te_3-GeTe system.

No	Composition, mol %			State
	GeS_e2	In_2Te_3	GeT*e*	
1	90	10	0	glassy
2	85	15	0	glassy
3	80	20	0	glassy + crystalline
4	81	9	10	glassy
5	76.5	13.5	10	glassy
6	72	18	10	glassy
7	67.5	22.5	10	glassy + crystalline
8	80	0	20	glassy
9	72	8	20	glassy
10	68	12	20	glassy
11	64	16	20	glassy
12	60	20	20	crystalline
13	63	7	30	glassy
14	59.5	10.5	30	glassy
15	56	14	30	glassy + crystalline
16	54	6	40	glassy
17	51	9	40	glassy
18	48	12	40	crystalline
19	49.5	5.5	45	glassy
20	46.75	8.25	45	glassy + crystalline
21	45	5	50	glassy + crystalline
22	45	0	55	glassy
23	42.75	2.25	55	glassy + crystalline
24	42	0	58	glassy + crystalline
25	40	0	60	crystalline
26	36	4	60	crystalline
27	35	0	65	crystalline

In - 3N5 (Merck), are the raw materials utilized in the samples' synthesis. The pre-ground starting components are weighed on an analytical balance with an accuracy of ± 0.0002 g. The physicochemical properties of the source components, the intermediate phase, and the final phase have been matched with the syntheses' regime (temperatures, length of the isothermal steps, and heating rate between them). The examined system's maximum synthesis temperature for the glasses is 900 ± 10°C, with vibration agitation of the smelter added for 2 h. The melt is quenched in ice and water at 10 - 15°C per second after being tempered to 850 ± 10°C.

Differential thermal analysis (DTA) using a device from the F. Paulik-J. Paulik-L. Erdey system, manufactured by MOM-Hungary (with an accuracy of ± 5°C), has defined the glasses' characteristic temperatures (glass transition temperature T_g, crystallization temperature T_{cr}, and melting temperature T_m). At a residual pressure of about 1.10^{-3} Pa, the standard sample (α-Al_2O_3) and the material under investigation, in an amount of approximately 0.3 g, are added and sealed. The heating rate is 15°C min^{-1}.

XRD utilizes Cu-K_α radiation (Ni-filter, θ = 5 - 40°) on a TUR-M61 apparatus. The samples' surfaces are examined using a Phillips EM 4000 electron microscope.

The density (d) and microhardness (HV) of the proven glassy state samples are determined using the hydrostatic [20] and Vickers' [21] procedures. Toluene is employed as the working liquid for the hydrostatic measurements as it wets the material well, does not dissolve it, and does not react with it. For the measurements, an analytical balance with an accuracy of ± 0.0002 g is used. Density is determined as the average of 10 measurements. For microhardness measurements, a 10 g load is applied to a metallographic microscope MIM-7 with an integrated microhardness meter PMT-3. The average of 20 measurements per sample serves as the working value for HV. The density and microhardness are measured with an accuracy of ± 5 %. The following formulas are used to determine the modulus of elasticity (E) [22], the minimal volume of the microvoids (V_h) [22], energy for their formation (E_h) [22], Hruby's criteria (K_G) [23], and compactness (C) [24].

$$V_h = 5.04 \cdot 10^{-3} \cdot \frac{T_g}{HV} \ [nm^3] \quad (1)$$

where T_g - glass transition temperature, HV - microhardness.

$$E_h = 29.75\ T_g,\ J\ mol^{-1}\ (T_g \rightarrow [K]) \quad (2)$$

where T_g - glass transition temperature.

$$E = 0.147\ HV,\ GPa \quad (3)$$

where HV - microhardness.

$$K_G = \frac{T_{cr} - T_g}{T_m - T_{cr}} \quad (4)$$

where T_g - glass transition temperature, T_{cr} - crystallization temperature, T_m - melting temperature.

$$C = d\left\{\sum_i \frac{M_i x_i}{d_i} - \sum_i \frac{M_i x_i}{d} - \right\}\left[\sum_i M_i x_i\right]^{-1} \quad (5)$$

where M_i, x_i, and d_i are the molar weight, molar part, and density of the i^{th} component, respectively; d is the sample's density.

Because of the linear nature of the $V_h(T_g, HV)$, $E_h(T_g)$, $E(HV)$, $K_G(T_g, T_{cr}, T_m)$ and $C(d)$ dependences, the error estimate of V_h, E_h, E, K_G, and C are the same as that of temperature characteristics, density, and microhardness.

RESULTS AND DISCUSSION

The synthesized bulk samples of the $GeSe_2$-In_2Te_3-GeTe system exhibit a shell-like surface, a pronounced luster, and a black colour.

Several compositions are typical glasses, characterized by the absence of peaks on the diffractograms, as indicated by the X-ray diffraction results (typical diffractogram Fig. 1, line A); these compositions comprise the glass-forming region. Other compositions exhibit small-intensity diffraction peaks with compositions located on the boundary of the zone; a typical diffractogram is presented in Fig. 1, line B. The third type of diffractograms characterizes the crystalline samples, which exhibit prominent peaks on their diffractograms, indicating that they are not within the glass-forming area; a typical diffractogram is presented in Fig. 1, line C.

According to the electron microscopic observation, the samples from the glass area exhibit a smooth and homogeneous surface. In contrast, the samples from the glass-forming boundary display tiny crystalline areas

on their surface. The crystalline samples have a rough surface devoid of any areas associated with a glassy phase.

Based on the syntheses carried out and the results obtained from the visual, X-ray diffraction, and electron microscopic analyses, we outline the region of glass formation in the three-component $GeSe_2$-In_2Te_3-GeTe system (Fig. 2).

It lies partially on the $GeSe_2$-GeTe (0 to 58 mol % GeTe) and the $GeSe_2$-In_2Te_3 sides (0 to 20 mol % In_2Te_3) from Gibbs's concentration triangle. The maximum solubility of In_2Te_3 in the glasses is ≈ 25 mol %.

S. Surinach et al. have investigated the $GeSe_2$-GeTe side [25]. They define the borders of glass formation on this site as up to 52 mol % GeTe. We have synthesized a few more compositions and enlarged the boundary to 58 mol %.

Table 2 summarizes the DTA analysis-determined samples' thermal properties, glass transition temperature T_g, crystallization temperature T_{cr}, and melting temperature T_m. Fig. 3 displays a few typical derivatogram samples. The thermograms demonstrate the various effects. The first is related to the temperature at which the glass transition occurs (i.e., the change in the angle coefficient of the temperature-time dependence); the second is exothermal and has a well-expressed maximum; the third effect is endothermal and results from the melting of a phase or solid solution that has already crystallized.

The authors mentioned above [25] have also investigated the thermal characteristics of the glasses on the $GeSe_2$-GeTe side, which we decided to use as comparative data for our measurements; these values are marked in Table 2.

The glass transition temperature strongly depends on the glass's composition. The $T_g(m)$ dependence at z = const lightly decreases, Table 2 $((GeSe_2)_x(In_2Te_3)_y(GeTe)_z$, m = y/(x+y)).

S. Surinach et al. have given one crystallization temperature (T_{cr}) for the compositions on the $GeSe_2$-GeTe side [25]. The crystallized alloys are rich in $GeSe_2$, and the addition of GeTe decreases T_{cr} (Table 2). The low-temperature exoeffects at 350 ± 5°C are related to the crystallization of the In_2Te_3 compound. They are practically uninfluenced by the increase in the In_2Te_3 content. These effects appear with the first added quantity of In_2Te_3.

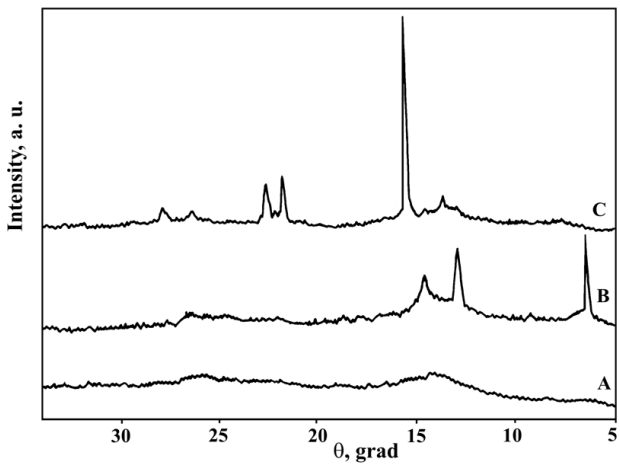

Fig. 1. Typical diffractograms of samples from the $GeSe_2$-In_2Te_3-GeTe system: A- composition $(GeSe_2)_{54}(In_2Te_3)_6(GeTe)_{40}$ (in the glass-forming region); B- composition $(GeSe_2)_{56}(In_2Te_3)_{14}(GeTe)_{30}$ (on the glass-forming boundary); C- composition $(GeSe_2)_{40}$ $(GeTe)_{60}$ (outside the glass-forming region).

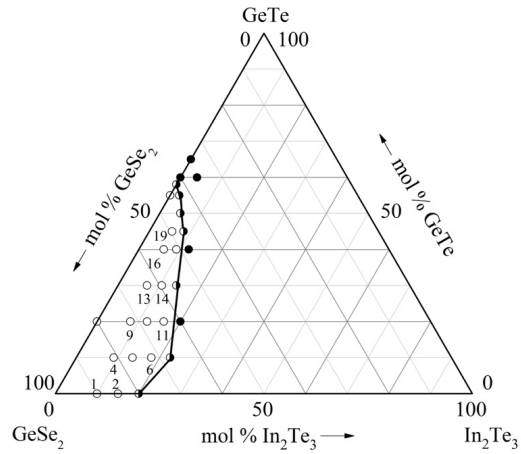

Fig. 2. Glass-forming region in the $GeSe_2$-In_2Te_3-GeTe system.

Significantly more complicated is the nature of the exoeffects in the temperature interval 395 - 410°C at a concentration of $In_2Te_3 \geq 10$ mol %. Two factors influence the crystallization temperature values. On the one hand, there are processes related to the crystallization of the In_2Te_3 and GeTe compounds, as their crystallization ability slightly depends on both GeTe and In_2Te_3. Nevertheless, the deviation of In_2Te_3 is ~ 5 mol %. On the other hand, with the increase of the GeTe content, the crystallization temperature considerably decreases (around 10°C with ~ 10 mol % decrease of the GeTe content), which gives us the reason

Table 2. Thermal properties and Hruby's criteria of glassy phases with composition $(GeSe_2)_x(In_2Te_3)_y(GeTe)_z$, where m = y/(x + y) and x + y + z = 100 mol %.

Composition, mol %			m	T_g, °C	T_{cr}, °C	T_m, °C	K_G
x	y	z					
100	0	0	0	394 [19]	504 [19]	744 [19]	0.458
90	10	0	0.1	323	405, 467	472, 592	0.439
85	15	0	0.15	305	395	486,601	0.437
90	0	10	0	377 [19]	473 [19]	713 [19]	0.400
81	9	10	0.1	313	405	587	0.506
72	18	10	0.2	280	352, 438	472, 606	0.284
80	0	20	0	364 [19]	461 [19]	648 [19]	0.519
72	8	20	0.1	285	409, 448	515, 577	0.738
64	16	20	0.2	260	367, 433	395, 462, 592	0.476
70	0	30	0	344 [19]	452 [19]	626 [19]	0.621
63	7	30	0.1	275	419	501, 553	1.075
59.5	10.5	30	0.15	246	352, 395	477, 505	0.693
60	0	40	0	322 [25]	437 [25]	569 [25]	0.871
54	6	40	0.1	241	347, 424	491, 515	0.631
55	0	45	0	312 [25]	413 [25]	538 [25]	0.808
49.5	5.5	45	0.1	217	347, 405	457, 481, 534	0.695

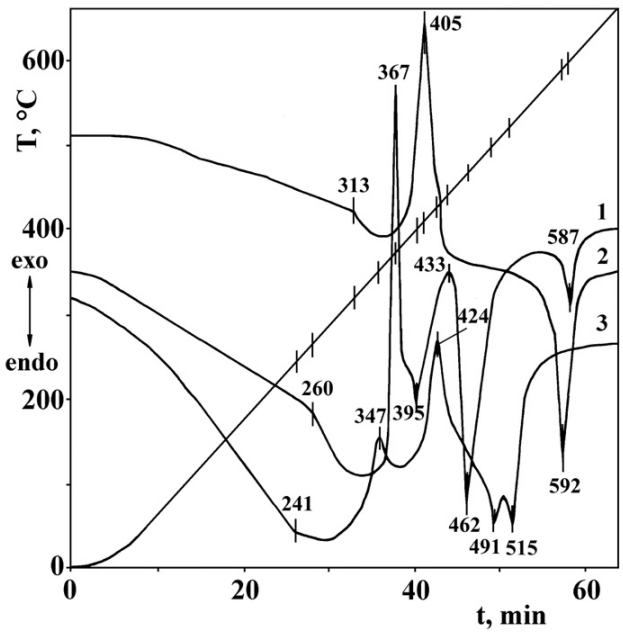

Fig. 3. Typical thermograms of samples from the $GeSe_2$-In_2Te_3-GeTe system: 1- sample with composition $(GeSe_2)_{64}(In_2Te_3)_{16}(GeTe)_{20}$; 2- sample with composition $(GeSe_2)_{81}(In_2Te_3)_9(GeTe)_{10}$; 3- sample with composition $(GeSe_2)_{54}(In_2Te_3)_6(GeTe)_{40}$.

to suggest that crystallizes not the pure $GeSe_2$ compound, but an alloy in which In_2Te_3 is present and with a high quantity of GeTe.

The melting temperature (T_m) varies from 395 to 744°C (Table 2). At m = const and with the increase of the GeTe content, T_m decreases. A minimum $T_m(z)$ dependence at m = 0.1 is observed, most probably due to the above-described factors. This assumption seems logical since, with the increase of the GeTe in the binary $GeSe_2$-GeTe system, the liquidus line goes through a minimum at about 45 mol % GeTe.

The presence of more than one melting temperature is logical and most probably related to the different melting points of already crystallized phases.

The subtraction $T_{cr} - T_g \geq 100$°C for some glasses (Table 2). This disparity determines their stability. Hrubi's criterion, which represents the glass-forming ability (Eq. 4), is a more precise metric for assessing the compound's effect on the glass-forming capability (Table 2). The high K_G values indicate significant obstructions in the nucleus formation and crystal formation processes. With the increase of the GeTe content (at m = const),

Table 3. Physical and thermomechanical properties of glassy phases with composition $(GeSe_2)_x(In_2Te_3)_y(GeTe)_z$.

Composition, mol %			m	T_g, K	HV, kgf mm^{-2}	d, g cm^{-3}	E, GPa	E_h, kJ mol^{-1}	V_h, 10^{-3} nm^3	C
x	y	z								
90	10	0	0.1	596	96	4.11	14.11	17.73	31.29	-0.1472
85	15	0	0.15	578	94	4.78	13.82	17.20	30.99	-0.0272
81	9	10	0.1	586	95	4.22	13.97	17.43	31.09	-0.1393
72	18	10	0.2	553	84	4.90	12.35	16.45	33.18	-0.0326
72	8	20	0.1	558	95	4.31	13.97	16.60	29.60	-0.1370
64	16	20	0.2	533	82	5.00	12.05	15.86	32.76	-0.0270
63	7	30	0.1	548	95	4.52	13.97	16.30	29.07	-0.1127
59.5	10.5	30	0.15	519	91	5.00	13.38	15.44	28.74	-0.0309
54	6	40	0.1	514	93	4.64	13.67	15.29	27.86	-0.1084
49.5	5.5	45	0.1	490	90	4.68	13.23	14.58	27.44	-0.1109

K_G increases, which is most probably related to the modifying properties of GeTe. This tendency can be expected since GeTe is an analog of $GeSe_2$, which can be obtained in the glassy state, even if it is hard. The $K_G(m)$ dependences at z = const show a well-expressed tendency of going through a maximum at $m \approx 0.1$, which means that at In_2Te_3 concentrations above 10 mol %, the building in of trigonal pyramids $InTe_{3/2}$ in the glass' carcass, built by $GeSe_{4/2}$ tetrahedrons, weakens the crystallization ability of the glasses.

Table 3 presents the results from the investigation of the physical (HV and d) and the calculation of the thermomechanical properties (V_h and E_h), as well as the elasticity modulus E and the compactness C.

The addition of GeTe (at m = const) and In_2Te_3 (at z = const) leads to an increase in the density, as this dependence is stronger when In_2Te_3 is added (Table 3). The density increase is logical since $d_{GeTe} > d_{In_2Te_3} > d_{GeSe_2}$ (6.2 > 5.75 > 4.6 g cm^{-3}). The stronger influence of In_2Te_3 at z = const is due to a partial exchange of Ge- and Se-atoms with the heavier indium and tellurium atoms.

From the analysis of the concentration dependencies $HV(m)_{z = const}$ and $HV(z)_{m = const}$, it can be concluded that the addition of In_2Te_3 and GeTe led to a weak decrease in the HV values. This is probably due to the relatively close microhardness values of the three initial components, which are in the following proportions: and $HV_{CeSe_2} > HV_{GeTe}$.

The energy required to generate micro-voids follows the path of T_g and varies from 3840 to 5000 kJ mol^{-1} (Table 3).

At a constant value of m, adding GeTe breaks the interlaced bonds of the Se-atoms and changes the void's configuration due to the building in of linear fragments -Ge-Te-. As a result of these structural changes, the minimal micro-void volume V_h slightly decreases. Adding In_2Te_3 at a constant concentration of GeTe also leads to structural changes, but their mechanism is different. Since the change of one Ge- and two Se-atoms with two In- and three Te-atoms will inevitably lead to the sum of two effects: breaking of interlaced bonds of Se-atoms, on the one hand, and three-dimensional netting of the structure, on the other, since the indium atoms are three-valent. The result of these structural changes is a weak increase in V_h.

Compactness (C) refers to the degree of structural densification in a glass, indicating how tightly the constituent atoms or structural units (e.g., Ge–Se, Ge–Te, In–Te bonds) are packed within the amorphous network. It slightly increases with the increase in In_2Te_3 content, as three atoms (Ge + 2Se) are replaced by five atoms with larger atomic radii (2In + 3Te). Since the samples with compositions on the m = 0.15 and m = 0.20 sections are near the glass-formation boundary, i.e., the possibility of crystallization increases, the compactness does not depend on the In_2Te_3-content and is nearly zero.

The elasticity modulus follows the path of HV and changes within the limits 594 - 1270 kgf mm^{-2} (Table 3).

CONCLUSIONS

New chalcogenide samples are synthesized, and the glass-forming region of the $GeSe_2$-In_2Te_3-GeTe system is delineated. It is situated partially on the $GeSe_2$-GeTe (0 to 58 mol % GeTe) and the $GeSe_2$-In_2Te_3 (0 to 20 mol % In_2Te_3) sides of the concentration triangle.

Thermal characteristics are determined. The glass transition and crystallization temperatures are in the ranges 217 - 394 °C and 347 - 504°C, respectively, and decrease as the In_2Te_3 content increases at a constant GeTe content. The melting temperatures range from 395 to 744°C. The density and microhardness are examined, ranging from 4.11 to 5.00 g cm^{-3} and 82 to 96 kgf mm^{-2}, respectively. At constant GeTe content, the addition of In_2Te_3 increases the density while reducing the microhardness. The characteristics of the mechanical and thermomechanical glassy phases, including modulus of elasticity, the minimal volume of microvoids, and their formation energy, are investigated. Hruby's criteria and compactness are calculated to determine glass-forming ability and degree of densification of the glasses. A hypothesis for its explanation is established, and a relationship between these characteristics and the make-up of the glasses from the system under study is established.

Acknowledgement

In gratitude to Prof. Venceslav Vassilev.

Author's contributions

All studies described in the manuscript were prepared by L. A.

REFERENCES

1. V.S. Minaev, Glassy semiconductor alloys, Metallurgy, Moscow, 1991, (in Russian).
2. Applications of chalcogenides: S, Se, and Te, Ed. Gurinder Kaur Ahluwalia, Springer, Springer International Publishing, Switzerland, 2017, 39.
3. R. Huang, L. Jiao, M. Li, Z. Dachuan, Effect of dilute tellurium and selenium additions on the high-temperature oxidation resistance of copper alloys, Oxid. Met., 89, 2018, 141-149. https://doi.org/10.1007/s11085-017-9793-6.
4. R. Kemparaju, Rohit, A. Prabhudesai, S. Charan Prasanth, M. Madesh Kumar, K. Ramesh, Electrical switching and phase change properties of GeTe-Al_2Te_3 chalcogenide alloys, Ceram. Int., 51, 15, B, 2025, 29046-29054. https://doi.org/10.1016/j.ceramint.2025.04.110.
5. S. Joshi, J.D. Rodney, N.K. Udayashankar, Peculiarities of electrical switching and phase transition dynamics in bismuth-infused Se-Te chalcogenide glasses: from bulk to thin film devices, ACS Appl. Electron. Mater., 6, 5, 2024, 3574-3588.
6. K. Ramesh, P. Pumlinmunga, R. Venkatesh, N. Naresh, E.S.R. Gopal, Phase change properties of chalcogenide glasses - some interesting observations, Key Eng. Mater., 702, 2016, 37-42.
7. N. Ciocchini, M. Laudato, M. Boniardi, E. Varesi, P. Fantini, A.L. Lacaita, D. Ielmini, Bipolar switching in chalcogenide phase change memory, Sci. Rep., 6, 2016, 29162. https://doi.org/10.1038/srep29162.
8. A. George, D. Sushama, S. Asokan, Electrical switching studies of bulk Ge-Te-In chalcogenide glasses, AIP Conference Proceedings, Optics: Phenomena, materials, 2011, Calicut, Kerala, India, 1391, 1, 2011, 778-780.
9. D. Cai, Y. Xie, X. Guo, P. Wang, L. Tong, Chalcogenide glass microfibers for mid-infrared optics, Photonics, 8, 11, 2021, 497. https://doi.org/10.3390/photonics8110497.
10. V.S. Shiryaev, A.P. Velmuzhov, T.V. Kotereva, E.A. Tyurina, M.V. Sukhanov, E.V. Karaksina, Recent achievements in development of chalcogenide optical fibers for mid-IR sensing, Fibers, 11, 6, 2023,54. https://doi.org/10.3390/fib11060054.
11. V. Shiryaev, E. Karaksina, T. Kotereva, A. Velmuzhov, A. Plekhovich, E. Boyko, Development of high-purity REE-roped chalcogenide glasses and fibers for mid-IR optical applications, Proceedings of 21st International Conference on Transparent Optical Networks (ICTON), Angers, France, 2019, 1-4. doi: 10.1109/ICTON.2019.8840498.
12. B. Bureau, C. Boussard-Plédel, S. Cui, R. Chahal, M.-L. Anne, V. Nazabal, O. Sire, O. Loréal, P. Lucas, V. Monbet, J.-L. Doualan, P. Camy, H. Tariel, F. Charpentier, L. Quetel, J.-L. Adam, J. Lucas, Chalcogenide optical fibers for mid-infrared sensing, Opt. Eng., 53, 2, 2014 027101/1-027101/7.

13. J. Troles, G. Renversez, Chalcogenide microstructured optical fibers: fabrication and applications, Proceedings of 24th International Conference on Transparent Optical Networks (ICTON), Bari, Italy, 2024, doi: 10.1109/ICTON62926.2024.10647513.
14. J. Nishii, S. Morimoto, R. Yokota, T. Yamagishi, Transmission loss of Ge-Se-Te and Ge-Se-Te-Tl glass fibers, J. Non-Cryst. Solids, 95-96, 2, 1987, 641-646.
15. C. Jiang, X. Wang, Q. Zhu, Q. Nie, M. Zhu, P. Zhang, S. Dai, X. Shen, T. Xu, C. Cheng, F. Liao, Z. Liu, X. Zhang, Improvements on the optical properties of Ge-Sb-Se chalcogenide glasses with iodine incorporation, Infrared Phys. Technol., 73, 2015, 54-61. https://doi.org/10.1016/j.infrared.2015.09.001.
16. A. Cui, Y. Wang, M. Wu, S. Dai, C. Lin, Z. Wu, L. Jiang, Ge-As-S chalcogenide glasses with high laser-induced damage threshold at 1.55 μm for acousto-optic applications, Ceram. Int., 51, 2025, 8816-8823.
17. I. Inagawa, R. Ilzuka, T. Yamagishi, R. Yokota, Optical and thermal properties of chalcogenide Ge-As-Se-Te glasses for IR fibers, J. Non-Cryst. Solids, 95-96, 1987, 801-808.
18. X. Liang, K. Jiao, X. Wang, N. Si, T. Xu, M. Zhong, Z. Zhao, X. Wang, J. Liu, P. Zhang, Y. Liu, Q. Nie, R. Wang, Ultra-high germanium-contained Se-chalcogenide glass fiber for mid-infrared, Infrared Phys. Technol., 104, 2020, 103112. https://doi.org/10.1016/j.infrared.2019.103112.
19. J. Gu, X. Shen, G. Jia, K. Xia, M. Wu, Z. Liu, Optical properties of Ge-Ga-Ag-Te high refractive index chalcogenide glasses, Opt. Mater. Express13, 5, 2023, 1320-1327, https://doi.org/10.1364/OME.484948.
20. P. Hidnert, E.L. Peffer, Density of solids and liquids, National Bureau of Standards Circular, 487, 1950, 3.
21. P. Moore, G. Booth, 9 - Mechanical testing of welds, in: P. Moore, G. Booth (Eds.), The welding engineer's guide to fracture and fatigue, Woodhead Publishing, Elsevier, 2015, p. 134. https://doi.org/10.1533/9781782423911.2.113.
22. V. Vassilev, G. Vassilev, E. Fidancevska, Thermo-mechanical characteristics of chalcogenide glasses, Chalcogen. Lett., 5, 12, 2008, 415-422.
23. L. Aljihmani, T. Hristova-Vasileva, K. Petkov, D. Nesheva, V. Vassilev, Thermomechanical characteristics of chalcogenide glasses from the $GeSe_2$-GeTe-PbTe system, Indian J. Eng. Mater. Sci., 9, 6, 2013, 234-238.
24. L. Aljihmani, K. Petkov, V. Vassilev, Glass forming region in the $GeSe_2$-GeTe-PbTe system and some physicochemical properties of glassy alloys, J. Non-Cryst. Solids, 358, 2012, 364-367.
25. S. Surinach, M.D. Baro, M.T. Clavaguera-Mora, N. Clavaguera, Glass formation and crystallization in the $GeSe_2$-GeTe-Sb_2Te_3 system, Thermochim. Acta, 133, 1988, 287-292.